Electron-Mediated Relaxation Following Ultrafast Pumping of Strongly Correlated Materials: Model Evidence of a Correlation-Tuned Crossover between Thermal and Nonthermal States

B. Moritz,[1,2,3,*] A. F. Kemper,[1] M. Sentef,[1] T. P. Devereaux,[1] and J. K. Freericks[4]

[1]*Stanford Institute for Materials and Energy Sciences, SLAC National Accelerator Laboratory, Menlo Park, California 94025, USA*
[2]*Department of Physics and Astrophysics, University of North Dakota, Grand Forks, North Dakota 58202, USA*
[3]*Department of Physics, Northern Illinois University, DeKalb, Illinois 60115, USA*
[4]*Department of Physics, Georgetown University, Washington, DC 20057, USA*

We examine electron-electron mediated relaxation following ultrafast electric field pump excitation of the fermionic degrees of freedom in the Falicov-Kimball model for correlated electrons. The results reveal a dichotomy in the temporal evolution of the system as one tunes through the Mott metal-to-insulator transition: in the metallic regime relaxation can be characterized by evolution toward a steady state well described by Fermi-Dirac statistics with an increased effective temperature; however, in the insulating regime this quasithermal paradigm breaks down with relaxation toward a nonthermal state with a complicated electronic distribution as a function of momentum. We characterize the behavior by studying changes in the energy, photoemission response, and electronic distribution as functions of time. This relaxation may be observable qualitatively on short enough time scales that the electrons behave like an isolated system not in contact with additional degrees of freedom which would act as a thermal bath, especially when using strong driving fields and studying materials whose physics may manifest the effects of correlations.

Optical reflectivity [1–5], photoemission spectroscopy [1,6–16], and resonant x-ray scattering [17–19] are equilibrium methods which in the time domain are ideally suited to studying dynamics of novel ordered phases or collective excitations [2–6,8–10,12–19]. On sufficiently short time scales, the initial recovery in these systems following an ultrafast pump pulse should be dominated by electron-electron scattering which on its own can drive the system into a new steady state. Conventional analysis has been based on a quasithermal paradigm ("hot electron" or multitemperature models) [20,21]; however, there have been few tests of the validity of its underlying assumptions as a function of the strength of electronic correlations [22], in particular as one tunes between the two regimes of a metal-to-insulator transition (MIT) [23].

The MIT driven by electronic correlations usually is accompanied by a number of interesting ordering phenomena among the spin, charge, and orbital degrees of freedom in a material. An understanding of the key physics which leads to these emergent phases is often at the heart of pump-probe experiments in condensed matter systems, including high-T_c cuprate superconductors [24], nickelates, manganites, ruthenates, vanadates [23], and even organic materials [25–27]. A number of experimental parameters can be used to tune across the MIT including doping and chemical substitution, pressure, and applied fields. What can be learned about the underlying physics leading to these phases as a function of these key parameters requires an understanding of the proper paradigm in which to ask the relevant questions and conduct analysis

of experimental data. This is in addition to what can be learned by tuning the interaction parameters of model systems simulated in fermionic or bosonic cold atom mixtures and performing the experimental equivalent of time-resolved, pump-probe measurements [28–30].

To avoid approximate treatments of either interactions or applied fields, in this Letter we discuss the evolution of a system described in equilibrium by the spinless Falicov-Kimball (FK) model [31,32] in the uniform phase, which possesses a MIT, whose effective Hamiltonian is given by

$$H = -\frac{t^*}{2\sqrt{d}}\sum_{\langle ij \rangle}(c_i^\dagger c_j + \text{H.c.}) - \mu\sum_i c_i^\dagger c_i + U\sum_i w_i c_i^\dagger c_i.$$
(1)

This model describes itinerant conduction electrons hopping between lattice sites with an energy t^* and chemical potential μ that experience electron-electron interaction with another species of localized electrons distributed according to an annealed statistical ensemble with an occupation $w_i \in \{0, 1\}$ on each site. The model can be tuned through the Mott MIT at half-filling ($\mu = U/2$ and $\langle w_i \rangle = 0.5$) by adjusting the electron-electron interaction U with $U_{\text{MIT}} = \sqrt{2}t^*$.

We model the transient pump pulse as a spatially uniform, harmonic, electric field with a Gaussian envelope of the form $\mathbf{E}(t) = \mathbf{E}_{\text{max}}\cos(\omega_p t)\exp[-t^2/\sigma_p^2]$ [see the temporal profile shown in Fig. 1(a)] incorporated via the Peierls' substitution [33] in the Hamiltonian gauge. The temporal evolution is simulated using an exact,
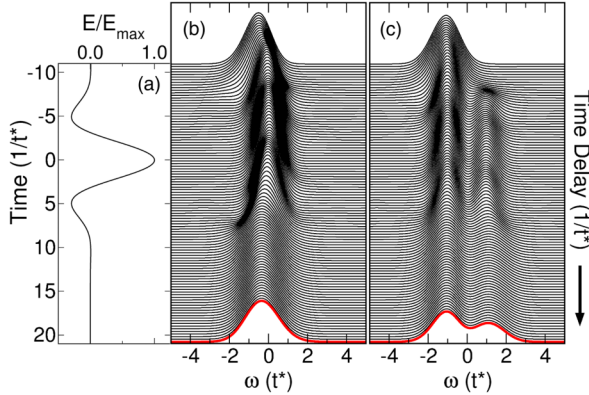
FIG. 1 (color online). (a) The electric field pump pulse that leads to the temporal evolution shown in panels (b) and (c) has a maximum intensity $E_{max} = 24E_0$ (normalized in the panel), modulation frequency $\omega_p = 0.5t^*$, and characteristic width $\sigma_p = 5/t^*$. (b),(c) Time-resolved pump-probe photoemission response for (b) metallic ($U = 0.5t^*$) and (c) insulating ($U = 2t^*$) systems determined for a probe pulse with characteristic width $\sigma_b = 2/t^*$. See the Supplemental Material [39] for a discussion of the evaluation of the photoemission cross section and the definition of the Gaussian probe pulse.

nonequilibrium formulation of dynamical mean-field theory [34–38] with the system initially started in thermal equilibrium at temperature $T = 0.1t^*$ prior to arrival of the pump pulse with an assumed polarization along the hyper-cubic body diagonal. Following standard convention, the energy unit is taken to be t^* throughout this Letter and the standard unit for time is $1/t^*$. Conversion to physical units, the effective electric field scale, denoted E_0, and details about the evaluation of the photoemission response, as well as an effective quasithermal response, can be found in the Supplemental Material [39].

Here we wish to understand, in general terms, how electron dynamics are affected by both strong fields and correlations; therefore, our exact treatment for this model is of more general interest than using a materials-specific Hamiltonian that may require a number of approximations to affect a full solution in the time domain. However, as a simplified model for correlated electrons, the FK model possesses an infinite set of constants of motion or constraints that vary with changes in the interaction strength U and temperature T. An important question concerns whether or not this simple model should thermalize at long times given these constraints. In this Letter, the applied pump pulse which drives the system out of equilibrium decays and leaves the Hamiltonian unchanged with respect to equilibrium. Hence, the system may be more amenable to thermal-ization than the case of a quantum quench [37] where the Hamiltonian changes discontinuously at time zero. The key issue of the present study is any sharp contrast which can be drawn in the thermalization of the itinerant degrees of freedom as a function of interaction strength.

Figures 1(b) and 1(c) show the characteristic photoemis-sion response [40–44] as a function of time delay for

representative metallic and insulating systems excited by the pump pulse shown in Fig. 1(a). The width of the photoemission probe pulse influences both the temporal resolution and energy resolution of the resulting spectrum, chosen here to strike a balance between the two.

For metallic correlations [Fig. 1(b), $U = 0.5t^*$] the pump pulse narrows and shifts the response toward the equilibrium Fermi level ($\omega = 0t^*$). Following the pump pulse, we observe a rapid relaxation toward a significantly broader spectral distribution characteristic of a new steady state. For stronger correlations on the insulating side of the Mott MIT [Fig. 1(c), $U = 2t^*$] the pump pulse narrows the response below the equilibrium Fermi level and transfers spectral weight across the insulating Mott gap (centered at the Fermi level). Similar to the behavior observed for weak correlations, we find a broader spectral distribution follow-ing the transient pump, although in this case a significant remnant spectral weight transfer across the gap persists, even in the long-time steady state. This rapid evolution following the decay of the pump pulse can be attributed to relaxation mediated by electron-electron scattering.

An increase in the effective temperature would naturally lead to broader features and a redistribution of weight across the insulating Mott gap, as the spectral function in equilibrium is temperature independent for this model. The long-time (bottom, red) traces in Fig. 1 can be used to assess whether the steady state is representative of the system in equilibrium at an elevated, effective temperature. However, as we now will show, our results highlight a distinct dichotomy in the temporal evolution as one tunes across the MIT. In the metallic regime the quasithermal picture remains valid with electron-electron mediated re-laxation characterized by evolution toward an effectively thermal steady state. However, tuning correlations across the MIT causes a breakdown in the quasithermal paradigm in the insulating regime with clearly nonthermal relaxation even at long times.

We first determine the appropriate temperature based on the change in total energy of the system [45]. Figure 2 shows the power delivered to the system by the pump pulse as well as the time-dependent total energy for the systems discussed in Fig. 1. Figures 2(c) and 2(d) show a compari-son between the total energy and the change in total energy determined by integrating the instantaneous power. As one can see, the simulation properly accounts for the energy delivered by the pump pulse with small deviations near time $0/t^*$ (near the center of the pulse) where the power (and instantaneous current) changes rapidly. This rapid variation in energy can be traced back to Bloch oscillations [46], like those observed for dc fields [36], although the oscillations are now ''chirped'' due to the time-varying field strength. The offset between the integrated power and total energy simply reflects the initial energy in equi-librium. Converting the total energy at long times to an effective temperature (assuming validity of the ''hot elec-tron'' model), we find an increase of $\sim 8\times$ for the weakly correlated, metallic system and $\sim 43\times$ for the strongly
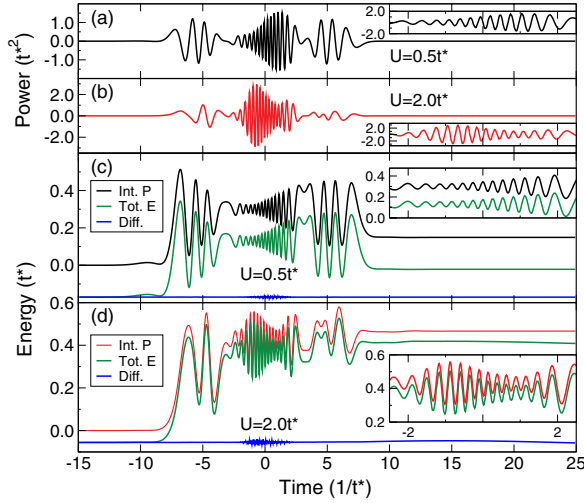
FIG. 2 (color online). Instantaneous power delivered to (a) metallic ($U = 0.5t^*$) and (b) insulating ($U = 2t^*$) systems discussed in Fig. 1. (c),(d) As a closed system, the change in total energy may be determined by integrating the instantaneous power [upper oscillating, black 2(c) or red 2(d) curves] or by direct calculation from the time derivative of the local propagator (lower oscillating, green curves). The constant offset (relatively flat, bottom, blue lines) represents the initial, equilibrium value in each case. The insets highlight times near the center of the pump pulse between $-2.5/t^*$ and $2.5/t^*$ that show rapid variation in each quantity.

correlated, insulating system for identical driving fields from the initial $T = 0.1t^*$.

Figure 3 shows the result of quasithermal fits to the photoemission response in both [3(a), $U = 0.5t^*$] the metallic and [3(b), $U = 2.0t^*$] insulating regimes. In each case the characteristic probe width is fixed as in Fig. 1. In the weakly correlated metal the simulated response closely matches that derived from the quasithermal fits with only small differences which grow upon increasing the pump strength and frequency as would befit simple expectations (see the Supplemental Material [39]). In this case the "best fit" also has been determined from a simple least-squares fit, but with a similar conclusion.

In contrast, the steady-state response in the insulating regime shows significant deviation from a quasithermal best fit, determined using either method, clearly indicating a breakdown in the "hot-electron" model. Issues associated with convergence of our self-consistent method restrict our studies to relatively strong driving fields; however, we can infer that similar observations should hold as the strength of the transient field is reduced, although the deviation from the quasithermal paradigm is likely to be noticeable only in the tail of the spectral function across the Fermi level, or, equivalently, the extracted, effective Fermi-Dirac distribution. Observations of nonthermal behavior already have been made experimentally for comparatively weaker driving fields [19].

We also examine the instantaneous electronic distribution providing a snapshot of the response to the applied
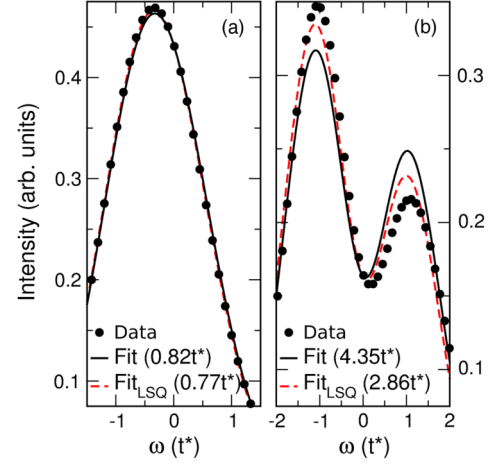

FIG. 3 (color online). Quasithermal fits of the steady-state photoemission response (characteristic probe width $\sigma_b = 2/t^*$) for (a) metallic ($U = 0.5t^*$) and (b) insulating ($U = 2t^*$) systems, respectively, with the effective temperature shown in parenthesis. The fits (solid black) are determined by extracting the temperature from the total energy, while the best-fit quasithermal response (dashed red) has been determined by the least-squares method (LSQ).

electric field and subsequent relaxation due to electron-electron scattering. Consider a simple noninteracting band metal. The initial distribution follows usual Fermi-Dirac statistics $f(\varepsilon_{\mathbf{k}} - \mu)$ with preferential occupation of the lower-energy states according to temperature. When driven by an electric field, an electron initially at momentum $\mathbf{k}$ shifts to $\mathbf{k} - e\mathbf{A}(t)$ (the standard Peierls' substitution). This behavior can be extracted directly from the gauge-invariant lesser Green's function for the system.

Consider the results shown in Fig. 4. Plotted versus the band energy $\varepsilon_{\mathbf{k}}$ and the normalized electron velocity $v_{\mathbf{k}} = \mathbf{v}_{\mathbf{k}} \cdot \hat{E}$, the line dividing the occupied and empty states rotates at a rate given by $-\partial \mathbf{A}(t)/\partial t \cdot \hat{E} = \mathbf{E}(t) \cdot \hat{E}$, simply the magnitude of the electric field as a function of time. One may remove this rotation by going over to an instantaneous frame which corresponds to examining the distribution functions in a particular gauge where one observes a static Fermi-Dirac distribution with no temporal dynamics. While the underlying physics remains unchanged, visualizing the results depends on whether one works with the gauged or gauge-invariant functions. We choose the latter (gauge-invariant formulation) as illustrated for a simple half-filled one-dimensional noninteracting band metal in Figs. 4(a)–4(d) and used to display the instantaneous electronic distribution functions for the metallic and insulating regimes shown in Figs. 4(e) and 4(f), respectively.

Incorporating the influence of interactions has a number of effects on the temporal behavior. First, the initial distribution broadens due to the electron-electron interactions, but remains independent of $v_{\mathbf{k}}$ and monotonically decreases as a function of $\varepsilon_{\mathbf{k}}$. The applied field drives particles via the Peierls' substitution, but now electron-electron scattering randomizes the distribution and eventually quenches Bloch
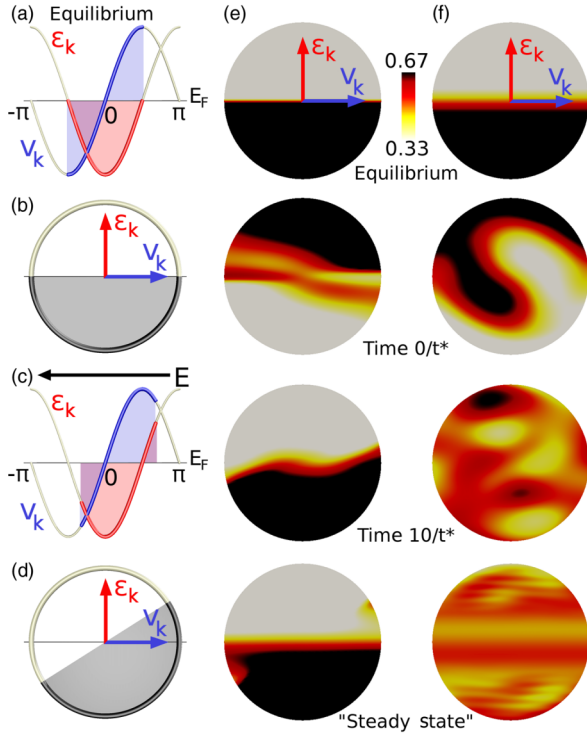
FIG. 4 (color online).   (a)–(d) A simple cartoon depicting the influence of an applied electric field on a noninteracting one-dimensional band metal at half-filling. (a),(c) The band energy ($\varepsilon_\mathbf{k}$, red highlight) and normalized band velocity ($v_\mathbf{k}$, blue highlight) distributions in equilibrium and under the influence of an applied electric field, respectively. In one dimension each band energy is associated with two band velocities [right ($+$) and left ($-$)]. In higher dimensions a distribution of velocities is associated with each band energy. (b),(d) The equivalent distribution shown in a two-dimensional band energy-velocity space with the axes labels annotated in each panel. The gray shading is a guide to the eye. (e),(f) Equal-time band energy-velocity distribution functions for the metallic ($U = 0.5t^*$) and insulating ($U = 2t^*$) regimes of Figs. 1(b) and 1(c), respectively, for various times (units of $1/t^*$). The band energy-velocity space spans a radius of $3.9t^*$ with the center of each plot at the origin ($0t^*$, $0t^*$) as indicated by the band energy-velocity axes in the top panels. A time-lapse sequence of images for both cases with finer resolution can be found in the Supplemental Material [39].

oscillations initially observable in the distribution function. After the pump pulse decays, electron-electron scattering drives the distribution toward a more-or-less static, steady-state, pattern. If the distribution depends on $v_\mathbf{k}$ or, as primarily observed in these simulations, no longer decreases monotonically as a function of $\varepsilon_\mathbf{k}$, one must question the validity of the quasithermal paradigm.

Figures 4(e) and 4(f) show the equal-time distribution function for a sequence of times in the metallic and insulating regimes, respectively. In Fig. 4(e) weak correlations allow the electric field pulse to easily shift the distribution function, similar to the expected behavior for a simple band metal. The system maintains a well-defined "Fermi edge," as observed in equilibrium, for all but those times with the strongest electric field near the center of the pulse

($0/t^*$). The edge reforms as the pump pulse decays and at the longest simulation times a significantly wider edge appears which agrees well with a simple Fermi-Dirac fit over a broad momentum range (see Supplemental Material [39]) indicative of the higher effective temperatures used to describe the observed photoemission response in Fig. 3.

In Fig. 4(f), electronic correlations on the insulating side of the Mott MIT produce an equilibrium distribution also with a well-defined "Fermi edge." These correlations provide an initial resistance to the influence of the applied pump pulse at short times and significantly scramble the electron redistribution at long times. Relaxation through electron-electron scattering induces a partial reformation of the edge at the longest simulation times; however, the system retains a nonthermal distribution of weight characterized primarily by a significant nonmonotonic dependence on $\varepsilon_\mathbf{k}$. A sequence of snapshots for both cases with finer time resolution and snapshots for the observed behavior with an alternative pump pulse can be found in the Supplemental Material [39].

These results reveal a dichotomy in the evolution of transiently excited electrons as one tunes across the Mott MIT in the FK model. The quasithermal picture, which has served to underpin much of the analysis for pump-probe experiments, remains essentially valid in the metallic regime where relaxation can be characterized by evolution toward an effectively thermal steady state. Tuning correlations to the insulating regime, across the MIT, causes a breakdown in this paradigm as one clearly observes relaxation toward a nonthermal state. In previous work on the Hubbard model in cold atom experiments [47], one observes an exponential increase in the effective relaxation time as a function of the interaction strength for a system prepared out of equilibrium with an excess number of double occupancies. For the short time scales considered here, this behavior in the Hubbard model is essentially consistent with our own observations. On short time scales where additional degrees of freedom, such as the lattice which provides new relaxation pathways, are less relevant, one should carefully consider the implications of this dichotomy. Interaction with these new degrees of freedom should dominate the much longer time recovery where the system must naturally return to its original equilibrium through coupling to the crystal lattice (electron-phonon coupling) and eventually ballistic and diffusive transport of the delivered pump energy to the material's bulk and subsequently the environment.

*moritz.physics@gmail.com

[1] U. Bovensiepen, J. Phys. Condens. Matter **19**, 083201 (2007).
[2] M. Rini, R. Tobey, N. Dean, J. Itatani, Y. Tomioka, Y. Tokura, R. W. Schoenlein, and A. Cavalleri, Nature (London) **449**, 72 (2007).
[3] D. Fausti, R. I. Tobey, N. Dean, S. Kaiser, A. Dienst, M. C. Hoffmann, S. Pyon, T. Takayama, H. Takagi, and A. Cavalleri, Science **331**, 189 (2011).
[4] S. Wall, D. Brida, S. R. Clark, H. P. Ehrke, D. Jaksch, A. Ardavan, S. Bonora, H. Uemura, Y. Takahashi, T. Hasegawa et al., Nat. Phys. **7**, 114 (2010).
[5] S. D. Conte, C. Giannetti, G. Coslovich, F. Cilento, D. Bossini, T. Abebaw, F. Banfi, G. Ferrini, H. Eisaki, M. Greven et al., Science **335**, 1600 (2012).
[6] L. Perfetti, P. A. Loukakos, M. Lisowski, U. Bovensiepen, H. Berger, S. Biermann, P. S. Cornaglia, A. Georges, and M. Wolf, Phys. Rev. Lett. **97**, 067402 (2006).
[7] A. L. Cavalieri, N. Müller, T. Uphues, V. S. Yakovlev, A. Baltuška, B. Horvath, B. Schmidt, L. Blümel, R. Holzwarth, S. Hendel et al., Nature (London) **449**, 1029 (2007).
[8] L. Perfetti, P. A. Loukakos, M. Lisowski, U. Bovensiepen, H. Eisaki, and M. Wolf, Phys. Rev. Lett. **99**, 197001 (2007).
[9] F. Schmitt, P. S. Kirchmann, U. Bovensiepen, R. G. Moore, L. Rettig, M. Krenz, J.-H. Chu, N. Ru, L. Perfetti, D. H. Lu et al., Science **321**, 1649 (2008).
[10] J. Graf, C. Jozwiak, C. L. Smallwood, H. Eisaki, R. A. Kaindl, D.-H. Lee, and A. Lanzara, Nat. Phys. **7**, 805 (2011).
[11] Y. Ishida, T. Togashi, K. Yamamoto, M. Tanaka, T. Taniuchi, T. Kiss, M. Nakajima, T. Suemoto, and S. Shin, Sci. Rep. **1**, 64 (2011).
[12] R. Cortés, L. Rettig, Y. Yoshida, H. Eisaki, M. Wolf, and U. Bovensiepen, Phys. Rev. Lett. **107**, 097002 (2011).
[13] L. Rettig, R. Cortés, S. Thirupathaiah, P. Gegenwart, H. S. Jeevan, M. Wolf, J. Fink, and U. Bovensiepen, Phys. Rev. Lett. **108**, 097002 (2012).
[14] J. A. Sobota, S. Yang, J. G. Analytis, Y. L. Chen, I. R. Fisher, P. S. Kirchmann, and Z.-X. Shen, Phys. Rev. Lett. **108**, 117403 (2012).
[15] C. L. Smallwood, J. P. Hinton, C. Jozwiak, W. Zhang, J. D. Koralek, H. Eisaki, D.-H. Lee, J. Orenstein, and A. Lanzara, Science **336**, 1137 (2012).
[16] S. Hellmann, T. Rohwer, M. Kalläne, K. Hanff, C. Sohrt, A. Stange, A. Carr, M. M. Murnane, H. C. Kapteyn, L. Kipp et al., Nat. Commun. **3**, 1069 (2012).
[17] M. Först, R. I. Tobey, S. Wall, H. Bromberger, V. Khanna, A. L. Cavalieri, Y. D. Chuang, W. S. Lee, R. G. Moore, W. F. Schlotter et al., Phys. Rev. B **84**, 241104 (2011).
[18] H. Ehrke, R. I. Tobey, S. Wall, S. A. Cavill, M. Först, V. Khanna, T. Garl, N. Stojanovic, D. Prabhakaran, A. T. Boothroyd et al., Phys. Rev. Lett. **106**, 217401 (2011).
[19] W. S. Lee, Y. D. Chuang, R. G. Moore, Y. Zhu, L. Patthey, M. Trigo, D. H. Lu, P. S. Kirchmann, O. Krupin, M. Yi et al., Nat. Commun. **3**, 838 (2012).
[20] S. Anisimov, B. L. Kapeliovich, and T. L. Perelman, Zh. Eksp. Teor. Fiz. **66**, 776 (1974) [Sov. Phys. JETP **39**, 375 (1974)].
[21] P. B. Allen, Phys. Rev. Lett. **59**, 1460 (1987).
[22] M. Eckstein and P. Werner, Phys. Rev. B **84**, 035122 (2011).
[23] M. Imada, A. Fujimori, and Y. Tokura, Rev. Mod. Phys. **70**, 1039 (1998).
[24] P. A. Lee, N. Nagaosa, and X.-G. Wen, Rev. Mod. Phys. **78**, 17 (2006).
[25] S. Lefebvre, P. Wzietek, S. Brown, C. Bourbonnais, D. Jérome, C. Mézière, M. Fourmigué, and P. Batail, Phys. Rev. Lett. **85**, 5420 (2000).
[26] B. J. Powell and R. H. McKenzie, Rep. Prog. Phys. **74**, 056501 (2011).
[27] A. Ardavan, S. Brown, S. Kagoshima, K. Kanoda, K. Kuroki, H. Mori, M. Ogata, S. Uji, and J. Wosnitza, J. Phys. Soc. Jpn. **81**, 011004 (2012).
[28] J. T. Stewart, J. P. Gaebler, and D. S. Jin, Nature (London) **454**, 744 (2008).
[29] R. Jördens, N. Strohmaier, K. Günter, H. Moritz, and T. Esslinger, Nature (London) **455**, 204 (2008).
[30] S. Trotzky, Y.-A. Chen, A. Flesch, I. P. McCulloch, U. Schollwöck, J. Eisert, and I. Bloch, Nat. Phys. **8**, 325 (2012).
[31] L. M. Falicov and J. C. Kimball, Phys. Rev. Lett. **22**, 997 (1969).
[32] J. K. Freericks and V. Zlatić, Rev. Mod. Phys. **75**, 1333 (2003).
[33] R. E. Peierls, Z. Phys. **80**, 763 (1933).
[34] A. Georges, G. Kotliar, W. Krauth, and M. J. Rozenberg, Rev. Mod. Phys. **68**, 13 (1996).
[35] J. K. Freericks, V. M. Turkowski, and V. Zlatić, Phys. Rev. Lett. **97**, 266408 (2006).
[36] J. K. Freericks, Phys. Rev. B **77**, 075109 (2008).
[37] M. Eckstein and M. Kollar, Phys. Rev. Lett. **100**, 120404 (2008).
[38] M. Eckstein, M. Kollar, and P. Werner, Phys. Rev. Lett. **103**, 056403 (2009).
[39] See Supplemental Material at http://link.aps.org/supplemental/10.1103/PhysRevLett.111.077401 for information on the nonequilibrium methodology and physical scaling, the evaluation of the photoemission cross section, the estimation of the effective temperature and fits to the photoemission response, as well as several movies which show the evolution of the equal-time electron distribution for different interaction strengths and pump conditions.
[40] M. Eckstein and M. Kollar, Phys. Rev. B **78**, 245113 (2008).
[41] J. K. Freericks, H. R. Krishnamurthy, and T. Pruschke, Phys. Rev. Lett. **102**, 136401 (2009).
[42] J. K. Freericks, H. R. Krishnamurthy, Y. Ge, A. Y. Liu, and T. Pruschke, Phys. Status Solidi B **246**, 948 (2009).
[43] M. Eckstein, M. Kollar, and P. Werner, Phys. Rev. B **81**, 115131 (2010).
[44] B. Moritz, T. P. Devereaux, and J. K. Freericks, Phys. Rev. B **81**, 165112 (2010).
[45] V. M. Turkowski and J. K. Freericks, Phys. Rev. B **73**, 075108 (2006).
[46] B. Moritz, T. P. Devereaux, and J. K. Freericks, Comput. Phys. Commun. **182**, 109 (2011).
[47] N. Strohmaier, D. Greif, R. Jördens, L. Tarruell, H. Moritz, T. Esslinger, R. Sensarma, D. Pekker, E. Altman, and E. Demler, Phys. Rev. Lett. **104**, 080401 (2010).